C/ebpα represses the oncogenic Runx3–Myc axis in p53-deficient osteosarcoma development

Kosei Ito (itok@nagasaki-u.ac.jp)
Nagasaki University https://orcid.org/0000-0002-8416-2466
Keisuke Omori
Shohei Otani

Article

Keywords:

Posted Date: October 11th, 2022

DOI: https://doi.org/10.21203/rs.3.rs-2103215/v1

Version of Record: A version of this preprint was published at Oncogene on July 4th, 2023. See the published version at https://doi.org/10.1038/s41388-023-02761-z.

Abstract

Osteosarcoma (OS) is characterized by *TP53* mutations in humans. In mice, loss of p53 triggers OS development, and osteoprogenitor-specific *p53*-deleted mice are widely used to study the process of osteosarcomagenesis. However, the molecular mechanisms underlying the initiation or progression of OS following or parallel to p53 inactivation remain largely unknown. Here, we examined the role of transcription factors involved in adipogenesis (adipo-TFs) in *p53*-deficient OS and identified a novel tumor suppressive molecular mechanism mediated by C/ebpα. C/ebpα specifically interacts with Runx3, a *p53* deficiency-dependent oncogene, and, in the same manner as p53, decreases the activity of the oncogenic axis of OS, Runx3-Myc, by inhibiting Runx3 DNA binding. The identification of a novel molecular role for C/ebpα in *p53*-deficient osteosarcomagenesis underscores the importance of the Runx-Myc oncogenic axis as a therapeutic target for OS.

Introduction

Osteosarcoma (OS) is a malignant bone tumor of mesenchymal cell origin, and there are few effective targeted therapies for the treatment of this malignancy. In humans, the frequent inactivation of *TP53* in sporadic OS[1,2] and its germline mutation in Li-Fraumeni syndrome, which shows a high incidence of OS[3], support the role of p53 as the critical tumor suppressor in osteosarcomagenesis. In mice, loss of p53 in osteoprogenitor or mesenchymal stromal cells (MSCs) is sufficient for OS development, which has been well-documented using the *Osterix (Osx)*/*Sp7*-Cre; $p53^{fl/fl}$ mouse line[4,5]. However, the molecular mechanisms underlying the initiation or progression of OS following or parallel to p53 inactivation remain largely unknown.

In a previous study, we identified the *p53* deficiency-dependent oncogenic role of Runx3, a member of Runx family of transcription factors (TFs), in OS development. In *p53*-deficient human and mouse OS, Runx3 is markedly upregulated and aberrantly upregulates Myc, the crucial oncogenic TF in OS[6], via the Runx consensus genomic element mR1 in the *Myc* promoter[7]. Because the DNA-binding ability of Runx3 is inhibited by p53 through a specific protein-protein interaction, Runx3 is considered a *p53* deficiency-dependent oncogenic TF in OS[7]. Concurrent loss of p53 and dysregulation of Myc, a pivotal tumor-promoting force in humans and mice[8], is mediated by the oncogenic Runx3. A better understanding of this fundamental mechanism could be achieved by identifying the tumor suppressive factors that inhibit the oncogenic mediator, Runx3.

In the present study, we examined the expression of TFs involved in adipogenesis (adipo-TFs) in *p53*-null OS cells. The differentiation of MSCs into adipocytes or osteocytes is thought to be mutually exclusive and tightly regulated by TFs[9–11]. Analysis of *Osx*-Cre; $p53^{fl/fl}$ mice (herein *OS* mice) and the TARGET (Therapeutically Applicable Research to Generate Effective Treatments) cohort, which possesses genomic alterations in the *TP53* gene, showed that adipo-TFs are not uniformly downregulated during osteosarcomagenesis. Some adipo-TFs serve as prognostic factors in human OS patients and their expression correlates with OS tumorigenicity, suggesting that they play tumor suppressive roles in OS.

Among them, a CCAAT/enhancer-binding protein, C/ebpα, was identified as the most favorable prognostic factor in human *p53*-deficient OS. Similar to Pparγ, C/ebpα is a master regulator of adipogenesis[10,12], and its function as a tumor suppressor gene has been reported in human cancers[13]. Repression of C/ebpα reduces the tumorigenic potential of OS cells in humans and mice.

Here, we provide a novel molecular mechanism in which C/ebpα acts as a tumor suppressor in *p53*-deficient osteosarcomagenesis. C/ebpα specifically interacts with Runx3, a *p53* deficiency-dependent oncogene, and decreases the activity of the oncogenic axis of OS, Runx3-Myc, by inhibiting Runx3 DNA binding. The anti-OS effects of C/ebpα examined all targeted Runx3, and inhibiting Runx3 reversed the functional defects of C/ebpα.

Results

C/ebpα is a favorable prognostic factor and is downregulated in p53-deficient osteosarcomagenesis

p53 inactivation is critical for the development and progression of OS in both humans and mice. The TARGET cohort possessing *TP53* alterations[7] and the transcriptome of bone marrow-MSCs (BM-MSCs, simply MSCs herein) and OS tissues obtained from *OS* mice were used for assessment. We compared the transcriptome of OS tissues to that of BM-MSCs (Fig. 1A) and analyzed changes in the expression of 45 adipo-TFs (Fig. 1B and Supplementary Fig. 1A). Of five adipo-TFs with significantly favorable or poor prognostic value in the human OS cohort (Fig. 1C and Supplementary Fig. 1B), C/ebpα, a favorable prognostic factor, was markedly downregulated in OS tissues that developed from *OS* mice, whereas the expression of the other four factors showed a moderate increase or decrease (Fig. 1B, D and Supplementary Fig. 1A). C/EBPα was different from other family members, including C/EBPβ, C/EBP , C/EBPδ, C/EBPε, and C/EBPζ, which showed no prognostic value in the *p53*-deficient human OS cohort (Fig. 1E). Based on these findings, the present study focused on the tumor suppressive function of C/ebpα.

C/ebpα is a tumor suppressor in p53-deficient osteosarcomagenesis in humans and mice

The tumor suppressive potential of C/ebpα *in vivo* was assessed by homozygous deletion of *C/ebpα* in *OS* mice, which shortened the lifespan and accelerated OS formation in *OS* mice (Fig. 2A, B). *C/ ebpα* depletion accelerated the onset of OS (Fig. 2B) and shortened the time from onset to death (Fig. 2C). Comparison of gene expression between BM-MSCs and OS cells isolated from OS tissues (mOS cells) showed differences in *C/ebpα* expression that were distinct from those of the other four prognostic factors (Fig. 2D). In *OS* mice, the tumorigenic potential of clonal mOS cells was inversely proportional to the expression level of C/ebpα (Fig. 2E). Exogenous expression of C/ebpα reduced the tumorigenicity of the mOS-1 cells listed in Fig. 2D (Fig. 2F). The *p53*-deficient human OS cell lines MG-63 and HS-Os-1, which endogenously express C/EBPα and have no tumorigenic potential in immunodeficient mice, became tumorigenic upon deletion of C/EBPα (Fig. 2G, H). These results indicate that C/ebpα is a tumor suppressor in osteosarcomagenesis in humans and mice.

C/ebpα depletion upregulates Myc and increases the tumorigenicity of p53-deficient MSCs

Cells of origin of OS are present in BM-MSCs carrying oncogenic gene alterations such as an inactive *p53*[14–16]. To evaluate the tumor suppressive role of C/ebpα in the development of *p53*-deficient OS, we isolated MSCs from *OS* mice and *OS*; *C/ebpα*$^{fl/fl}$ mice, and compared their tumorigenic potential. Deletion of C/ebpα strongly increased the tumorigenic potential of MSCs from *OS* mice (*OS*;*C/ebpα*$^{fl/fl}$ MSCs vs. *OS* MSCs) (Fig. 3A). The tumorigenicity of *OS* MSCs was dependent on Myc (Fig. 3A, B). This was confirmed by the finding that both *OS*; *Myc*$^{fl/+}$ MSCs and *OS*; *Runx3*$^{fl/fl}$ MSCs lacking Runx3, which upregulates Myc in the absence of p53[7], showed little tumorigenic potential (Fig. 3A, B). *OS* MSCs formed small tumors, some of which contained an osteoid matrix, whereas *OS*; *C/ebpα*$^{fl/fl}$ MSCs formed bigger and malignant tumors with higher levels of Myc expression in immunodeficient mice (Fig. 3C). Reintroduction of C/ebpα into *OS*; *C/ebpα*$^{fl/fl}$ MSCs decreased their tumorigenicity and downregulated Myc (Fig. 3D, E). *C/EBPα* deletion in MG-63 and HS-Os-1 cells upregulated MYC (Fig. 3F), and *C/EBP* and *MYC* expression was inversely correlated in the human OS cohort (TARGET) (Fig. 3G). These findings suggest that C/ebpα acts as a tumor suppressor by downregulating Myc in *p53*-null OS development.

Myc is suppressed by C/ebpα in various cell types, and different underlying mechanisms have been proposed[13]. C/ebpα represses E2Fs, which positively regulate Myc[17–19]. In addition, C/ebpα inhibits Rb-phosphorylation through an inhibitory protein-protein interaction with CDK2 and CDK4, thereby indirectly inhibiting E2Fs[20,21]. In the present study, we evaluated the contribution of E2Fs and Rb-phosphorylation to the Myc upregulation caused by loss of C/ebpα in the *p53*-deficient setting. Treatment with HLM006474, an E2F inhibitor[22], downregulated Myc as well as E2F4, a positive control for HLM006474 treatment in the presence of C/ebpα, but not Myc, which was upregulated in the absence of C/ebpα (Supplementary Fig. 2A). This suggests that although E2Fs upregulate Myc, the upregulation of Myc in the absence of C/ebpα in *p53*-deficient MSCs is independent from E2Fs. There is no significant correlation between inactivation of Rb and tumorigenicity of mOS cells in the development of *p53*-deficient OS[7]; consistently, we did not find an inverse association between Rb phosphorylation and Cebpα/CEBPα expression in mOS cells (Supplementary Fig. 2B, C), HS-Os-1 cells (Supplementary Fig. 2D), and MSCs (Supplementary Fig. 2E, F). Even in the presence of p53, C/ebpα deletion did not promote Rb phosphorylation in MSCs (Supplementary Fig. 2F). These results suggest that C/ebpα targets other factors essential for Myc regulation in the *p53*-null setting that are not E2Fs or Rb.

C/ebpα attenuates DNA binding of oncogenic Runx3 to mR1 in the absence of p53

C/ebpα physically interacts with Runx3, as it does with Runx1[23,24]. Similar to Runx1, Runx3 exhibited a stronger interaction with C/ebpα than Runx2 (Fig. 4A). In *OS* MSCs, the endogenous interaction of C/ebpα with Runx3 is stronger than that with Runx2 (Fig. 4B). Consistent with these results, in mOS cells, exogenously expressed C/ebpα inhibited the binding of Runx3 to mR1, an essential Runx consensus site in the *Myc* promoter for aberrant upregulation of Myc in the absence of p53[7], more significantly than the

binding of Runx2, as revealed by EMSA (Fig. 4C-E) and ChIP (Fig. 4F). A similar trend was observed when p53 was deleted from ST2, a mouse BM-MSC line, and C/ebpα was induced (Fig. 4G). In the absence of Runx3 or mR1, disruption of C/ebpα did not increase Myc and the tumorigenicity of *OS* MSCs, whereas in the presence of both, loss of C/ebpα increased Myc and tumorigenicity (Fig. 4H, I). These results indicate that C/ebpα attenuates Myc upregulation by blocking Runx3 DNA binding to mR1, thereby suppressing the tumorigenicity of *OS* MSCs.

The Runt domain, which is the DNA binding domain, was suggested as the interaction domain of Runx1 with C/ebpα[24,25], although this has not been clearly demonstrated. The interaction domain of Runx2 with C/ebpβ is a C-terminal domain but not the Runt domain[26]. A Runx3 polypeptide containing the Runt domain was confirmed to interact with C/ebpα (data not shown), as suggested by the inhibition of DNA binding by C/ebpα; however, the specific domain in Runx3 was not identified.

Loss of C/ebpα does not affect Myc regulation and osteosarcomagenesis in the presence of p53

C/ebpα suppresses oncogenic Runx3, which upregulates Myc via mR1 only in the absence of p53[7]. Consistent with this finding, in the presence of p53, loss of C/ebpα did not upregulate Myc in ST2 cells and MSCs (Fig. 5A, B), and inducible C/ebpα did not affect Myc expression levels in ST2 cells (Supplementary Fig. 3). As shown in Fig. 2A, osteoprogenitor-specific deletion of C/ebpα promoted *p53*-deficient OS development *in vivo*, whereas deletion of C/ebpα alone resulted in no tumor formation in mice and no difference in lifespan from control mice (Fig. 5C). In addition, MSCs isolated from *Osx*-Cre; *C/ebpα*$^{fl/fl}$ mice had no tumorigenicity t in immunodeficient mice (data not shown). All these findings suggest that C/ebpα functions as a tumor suppressor in OS development only in the absence of p53. As revealed by micro-CT (μCT) analysis, on the other hand, deletion of C/ebpα by *Osx*-Cre significantly increased trabecular and cortical bone formation in the adult femur, a common site of OS, although the trend was not observed for all parameters examined (Fig. 5D, E).

The Runx inhibitor AI-10-104 effectively cured p53**- and** C/ebpα**-deficient OS**

The tumor suppressor C/ebpα targets Runx3 in the development of *p53*-deficient OS. Treatment with the Runx inhibitor AI-10-104[27] downregulated Myc in both *p53*- and *C/ebpα*-negative MSCs (*OS*; *C/ebpα*$^{fl/fl}$ MSCs) (Fig. 6A) in a dose-dependent manner (Fig. 6B); however, its effect on Myc downregulation was smaller in *p53*-negative but *C/ebpα*-positive MSCs (*OS* MSCs) (Fig. 6A). These results demonstrate that induction of Myc by Runx3 is dependent on both p53 and C/ebpα deficiency. Correspondingly, administration of AI-10-104 had an obvious therapeutic effect on *OS*; *C/ebpα*$^{fl/fl}$ mice that developed lower extremity OS (Fig. 6C).

Taken together, the present results indicate that the oncogenic potential of Runx3, which aberrantly upregulates Myc, is suppressed by both tumor suppressors, p53 and C/ebpα, in normal MSCs. The *p53*-negative MSCs (*OS* MSCs) in which only C/ebpα attenuates Runx3 are considered to be in a pre-OS state.

Once C/ebpα is downregulated, unleashed Runx3 abnormally upregulates Myc and promotes osteosarcomagenesis (Fig. 6D).

Discussion

In mice, *C/ebpα* deletion promoted *p53*-deficient osteosarcomagenesis and conferred tumorigenicity on *p53*-deficient MSCs. In humans, *C/EBPα* was defined as a favorable prognostic factor for OS. The present data indicate that C/ebpα plays a tumor suppressor role in the development of OS. To the best of our knowledge, this study is the first to report *Osx*-positive MSC/osteoprogenitor-specific KO of C/ebpα, an adipo-TF, in mice. In the presence of p53, loss of C/ebpα modestly enhanced bone formation in adult mice without an oncogenic phenotype, suggesting that inhibition of adipogenesis by its deficiency resulted in a relative enhancement of osteogenesis, in line with the phenotype of systemic *C/ebpα*-deficient mice[28]. Although the tumor suppressive function of C/ebpα is not obvious in response to its mere deletion, it appears to function as an attenuator against a powerful oncogenic force, i.e., Myc dysregulation by Runx3 in the absence of p53, as if it were a substitute for p53.

Along with *TP53* mutations, genetic inactivation of *RB-1* plays a key role in human OS development[1]. In mice in which *p53* and/or *Rb* are deleted by *Osx*-Cre, OS development is dependent on loss of p53 but not Rb, whereas it is potentiated by loss of Rb[5,29,30], suggesting that E2Fs can promote *p53*-deficient osteosarcomagenesis. C/ebpα decreases the activity of E2Fs[13,31]. Moreover, C/ebpα inhibits Rb phosphorylation through direct interaction with Cdk2 and Cdk4, leading to Cdk/cyclin kinase inactivation[20,21]. Thus, the possible impact of loss of C/ebpα on Rb inactivation and/or E2F activation leading to progressive tumorigenicity in *OS* mice and *OS* MSCs needs to be examined in more detail. However, in this study, Myc upregulation caused by *C/ebpα* deficiency was not primarily dependent on Rb phosphorylation or E2F activity.

During normal differentiation, TFs of one lineage (osteogenesis) repress TFs of the other lineage (adipogenesis), thereby completing and maintaining the differentiation state[11]. During osteogenesis, adipo-TFs are generally downregulated; however, in abnormal osteogenesis, namely, osteosarcomagenesis, the tight regulation is disturbed. Among adipo-TFs, the downregulation of *C/ebpα* suggests that other oncogenic factors involved in OS development repress C/ebpα. Downregulation of *C/ebpα* by multiple mechanisms has been recognized in a variety of tumors: by microRNA (miR)-182 in acute myeloid leukemia development[32], by miR-101 in tumor-associated macrophages[33], epigenetically by hyper-methylation of the *C/ebpα* promoter in head and neck squamous cell carcinoma[34], by HIF-1 in breast cancer hypoxia[35], and by TGFβ in epithelial-to-mesenchymal transition mediating breast cancer metastasis[36]. Myc and C/ebpα may also form a negative regulatory loop, as suggested by a previous report that Myc represses C/ebpα expression in hibernoma cells[37]. In any case, oncogenic signaling pathways in the microenvironment of *p53*-deficient OS undoubtedly play an important role in C/ebpα downregulation.

In addition to C/EBPα, PPARγ, a master regulator of adipogenesis, was identified as the most favorable prognostic adipo-TF in the TARGET cohort analysis (Fig. 1C and Supplementary Fig. 1B), and its tumor suppressive roles in OS have been suggested[15,38]. The inhibitory regulation of Runx2, a master regulator of osteogenesis, by PPARγ has been documented in the context of adipogenic/osteogenic regulation[39]. Furthermore, the oncogenic role of Runx2 in the genesis of *p53*-deficient OS was previously suggested[7,40,41]. Therefore, although not examined in this study, PPARγ likely functions in a repressive manner against Runx2 and possibly Runx3 in the *p53*-deficient OS development.

The cooperative actions of C/ebps with Runx1 or Runx2 in hematopoiesis[23] or osteogenesis[26], respectively, have been reported. RUNX1 and C/EBPα act synergistically to increase M-CSF receptor expression via their respective binding sites, which are located adjacent to each other in the promoter of the *M-CSF* receptor[23]. Runx2 and C/ebpβ directly interact and synergistically increase osteocalcin expression via a C/ebp consensus site in the *osteocalcin* promoter[26]. In addition, Runxs and C/ebpα compete with each other for binding to an overlapping regulatory element in the promoter region of *CD11a* integrin in myeloid cells[42]. In contrast to these reports, this study demonstrated the inhibition of Runx3 DNA binding to mR1, an indispensable element (a Runx consensus site) in the *Myc* promoter for aberrant upregulation of Myc, by C/ebpα through direct protein-protein interaction. This is a previously unreported inhibitory interaction mode between Runxs and C/ebps as oncogenes and anti-oncogenes, similar to the aforementioned inhibitory interaction of E2Fs and C/ebpα, in undifferentiated proliferating cells such as MSCs or in tumorigenic cells lacking p53. In *p53*-deficient thymic lymphomagenesis, we recently reported that Runx1 shows oncogenic transactivation to upregulate Myc via mR1[43]. In *p53*-deficient T-cell lymphomas, the presence or absence of inhibition of Runx1 DNA binding by C/ebpα is also an interesting issue.

This manuscript emphasizes the essentiality of the oncogenic Runx3-Myc axis in *p53*-deficient osteosarcomagenesis by identifying a novel tumor suppressive role for C/ebpα. C/ebpα functions as an auxiliary brake against oncogenic Runx3 in case p53 inhibition is no longer effective as shown in Fig. 6D. The loss of C/ebpα causes the pre-OS to develop into OS. A Runx inhibitor was effective even in the absence of both tumor suppressors, p53 and C/ebpα. Runx is a very effective therapeutic target for OS.

Materials And Methods

Mouse lines

Floxed mouse lines of *p53*[44], *Runx3*[45], and *Myc*[46] and an mR1-mutated mouse line (*mR1*$^{m/m}$)[7] were described previously. *Sp7/Osx*-Cre (no.006361) and a floxed mouse line of *C/ebpa* (no.006230) lines were purchased from Jackson Laboratory. The line no. 006230, which originally possessed the *Mx1*-Cre gene, was backcrossed to remove it before crossing with the *Sp7/Osx*-Cre lines. All mouse studies were performed in the C57BL/6 background using approximately equal numbers of males and females. The details of all animal experiments, including the number of mice (sample size) to be used, were reviewed

and approved by the Animal Care and Use Committee of Nagasaki University Graduate School of Biomedical Sciences (no. 2104011709-2). Four mice were housed in each cage. Mice were reared in a pathogen-free environment on a 12 h light cycle at 22 ± 2°C.

BM-MSCs and mOS and human OS cells

All cells used in this study were confirmed to be free of mycoplasma infection and maintained in F12/DMEM supplemented with 10% fetal bovine serum. For the generation of BM-MSCs, BM cells were flushed from the femur of mice with F12/DMEM. Cd11b- and Cd45-negative adherent BM cells, which were negatively selected using a magnetic cell sorting system (MACS; Miltenyi Biotec) consisting of CD11b (no. 130-049-601) and CD45 (no. 130-052-301) MicroBeads and MS Columns (no. 130-042-201), were used as BM-MSCs. Similarly, for the generation of mOS cells, adherent cells obtained from mouse OS tissues that were minced and collagenase I-digested were negatively selected using a MACS. Cd11b- and Cd45-negative OS cells were used as mOS cells. ST2/HS-Os-1 and MG-63 were purchased from RIKEN and JCRB, respectively.

AI-10-104 (AOB17076; AOBIOUS) and HLM006474 (SML1260; Sigma-Aldrich) were used for inhibition of Runxs and E2Fs, respectively.

Genome editing for deletion of CEBPα/Cebpα **and** p53

For *CEBPα/Cebpa* deletion, HEK293T cells were cotransfected with a lentiCRISPRv2 plasmid (Addgene #52961) containing each sgRNA sequence (see below), the second-generation packaging plasmid psPAX2 (Addgene #12260), and the envelope plasmid pMD2.G (Addgene #12259) using the X-tremeGENE HP DNA Transfection Reagent (Roche). After filtration through a 0.45 μm filter, conditioned medium containing each lentivirus was used for infection. Infected cells were selected with puromycin. For *p53* deletion, lentiCRISPRv2 was replaced by lentiCRISPRv2-blast (Addgene #98293) and puromycin by blasticidin. Resistant cells were used without cloning. sgRNA sequences except the Scrambled control were extracted from the genome-scale GeCKO V2 libraries[47]. The sgRNA sequences used were as follows: Scrambled, 5'-TGGTTTACATGTCGACTAAC-3'; *CEBPα/Cebpa* h5, 5'-CAGTTCCAGATCGCGCACTG-3'; *CEBPα/Cebpa* h6, 5'-GAGCCCCTGTACGAGCGCGT-3'; *p53* m1, 5'-AGTGAAGCCCTCCGAGTGTC-3'; and *p53* m6, 5'-GTGCTGTGACTTCTTGTAGA-3'. For *Cebpa* deletion in MSCs, both sgRNA (h5 and h6) were used, but only *Cebpa*-deleted MSCs using h6, which showed a clearer depletion of the C/ebpα protein, were used. For *p53* deletion in ST2 cells, both sgRNA (m1 and m6) were used, but only *p53*-deleted ST2 cells using m1, which showed a stronger reduction of the p53 protein, were used.

Stable and inducible expression of exogenous genes

MSCs and mOS cells were retrovirally transfected with pMSCV-vector (Clontech/Takara) or pMSCV-mouse-C/ebpα, and selected using puromycin. Resistant cells were used without cloning. Expression of C/ebpα was induced in ST2 cells or *p53*-deleted (Δp53) ST2 cells using the Retro-X Tet-One Inducible Expression System (Clontech/Takara). Cells were retrovirally transfected with pRetroX-teton-mouse

C/ebpα and selected with puromycin. Resistant cells were treated with 100 ng/ml doxycycline (dox) for the indicated times.

RNA-seq

RNA was extracted from MSCs and mOS cells isolated from three individual *OS* mice using the NucleoSpin RNA kit. RNA quality was assessed on a Bioanalyzer (Agilent). Libraries were prepared using the TruSeq stranded mRNA Library Prep Kit (Illumina). Next-generation sequencing (NGS) libraries were sequenced as 100 bp paired end reads using MGI's DNBSEQ-G400RS, with an average of 40 million reads and an average mapping rate of 83%. RNA counts were quantified using Kallisto3 by pseudo-aligning FASTQ reads to the mouse genome (mm10). RNA-seq data generated and submitted to DDJB sequence read archive with the accession number DRA011168 in the last study[7] were used for OS tissues of *OS* mice.

In each of the three groups (MSCs, mOS cells, and OS tissues), genes were excluded from subsequent analyses if their average expression counts were zero. Principal component analysis was performed using the prcomp function of R. Differential expression analysis of OS tissues vs. MSCs was performed using DEseq2, and the results were used to draw both MA plots and heatmaps. Of 48 genes with overlapping Gene Ontology terms GO:0003700 (DNA binding TFs) and GO:0045444 (Fat Cell Differentiation), 45 orthologs between humans and mice were considered adipo-TFs in this study.

Gene expression microarray data and the corresponding clinical information from 89 primary OS patients were obtained from the TARGET project (https://ocg.cancer.gov/programs/target) under accession number phs000468 on NCBI dbGaP. Correlation analysis was performed using Spearman's correlation. For survival analysis, 86 datasets possessing both sequencing and clinical information were used. Hazard ratios were calculated with the Cox proportional hazard model after the patients were stratified into low- and high-expressing groups based on the median value for each gene.

Administration of Runx inhibitors

OS mice that developed OS in the lower limbs, the most frequent site, were selected blindly, and administration of the inhibitors via intraperitoneal injection was initiated when the onset of OS was visually confirmed (i.e., when the tumor was approximately 3 mm in diameter). AI-10-104 (AOB17076; AOBIOUS) was administered at 1 mg/kg in 100 µl of 10% DMSO in PBS, once every 3 or 4 days (twice a week) for 13 weeks (90 days) after OS onset.

Immunoblotting and immunoprecipitation

Lysates of OS cells and MSCs for immunoblotting were prepared using a lysis buffer containing 9 M Urea, 2% Triton X-100, 2-mercaptoethanol, and protease/phosphatase inhibitors. Immunoblotting was performed using the following antibodies: anti-Runx2 (D1H7; Cell Signaling Technology or R2-8G5; MBL), anti-Runx3 (D6E2; Cell Signaling Technology or R3-8C9; an in-house mouse monoclonal antibody[48]), anti-VWRPY (anti-pan-Runx) (Rp-6C2; an in-house mouse monoclonal antibody[7]), anti-c-Myc (ab32072;

Abcam), anti-C/ebpα (D56F10; Cell Signaling Technology), anti-p53 (DO-1; MBL, 1C12; Cell Signaling Technology), anti-Rb (sc-74562; Santa Cruz Biotechnology), anti-phospho-Rb (D59B7; Cell Signaling Technology), anti-E2F4 (sc-866; Santa Cruz Biotechnology), anti-histone H3 (ab1791; Abcam), and anti-β-actin (AC-15; Sigma-Aldrich). Whole-cell extracts of HEK293T cells transiently expressing human C/EBPα (pcDNA3.1- C/EBPα) and RUNX1, RUNX2, or RUNX3 (pcDNA3.1-RUNX1, -RUNX2, or -RUNX3) were immunoprecipitated with an anti-C/ebpα antibody (D56F10). The immunoprecipitates were subjected to immunoblotting using anti-VWRPY (Rp-6C2)/anti-C/ebpα (D56F10) antibodies. To detect endogenous protein interactions, immunoprecipitates of nuclear extracts (NEs) of *OS* MSCs generated using anti-Runx2 (D1H7), anti-Runx3 (D6E2) antibodies, or normal rabbit IgG were subjected to immunoblotting using anti-Runx2 (R2-8G5), anti-Runx3 (R3-8C9), or anti-C/ebpα (D56F10) antibodies.

Emsa

EMSA was performed using the LightShift Chemiluminescent EMSA Kit and Chemiluminescent Nucleic Acid Detection Module (Thermo Fisher Scientific). Each binding reaction (10 μl) contained 50 ng/μl poly (dI-dC), 75 fmol labeled probes, and NE in the buffer supplied in the kit. NE was prepared from mOS-1 cells, mOS-1 cells stably expressing C/ebpα (pMSCV-mouse c/ebpα) or harboring the pMSCV-vector, and 293T cells transiently expressing C/ebpα (pcDNA3.1-mouse C/ebpα) or harboring the pcDNA3.1-vector using the NE-PER Nuclear and Cytoplasmic Extraction Reagents (Thermo Fisher Scientific). The NEs of mOS-1 cells and labeled DNA probes with or without unlabeled probes were incubated at room temperature for 20 min and resolved on 5% polyacrylamide gels in 0.5× TBE buffer. For super-shift analysis, anti-Runx1 (an in-house polyclonal antibody[7]), anti-Runx2 (D1H7), anti-Runx3 (D6E2) antibodies, or rabbit normal IgG were added after the binding reaction and incubated at room temperature for an additional 10 min. The NE of C/ebpα- or mock-293T cells was incubated on ice for 10 min with the NE of mOS-1 cells, and then for 20 min at room temperature with labeled DNA probes. 5'-biotinylated labeled or unlabeled mR1, 5'-TTCCACCTGCGGTGACTGAT-3', or unlabeled mutated (mt) mR1, 5'-TTCCACCTGCCGTGACTGAT-3', were used as oligonucleotide probes.

ChIP

ChIP experiments were performed using the SimpleChIP Enzymatic Chromatin IP kit with magnetic beads (Cell Signaling Technology). Briefly, 6 million cells were cross-linked with 1% formaldehyde for 10 min at room temperature. After permeabilization, cross-linked cells were digested with micrococcal nuclease and immunoprecipitated with anti-Runx2 (D1H7; Cell Signaling Technology) or anti-Runx3 (D6E2; Cell Signaling Technology) antibody. Immunoprecipitated products were isolated with Protein G Magnetic Beads (Cell Signaling Technology) and subjected to reverse cross-linking. The DNA was subjected to quantitative PCR using the following primer pairs:

Mouse gene desert: 5'-ACCAAGCACAGAAAAGGTTCAAAC-3' and

5'-TCCAGATGCTGAGAGAAAAACAAC-3';

mR1: 5'-GCCTTAGAGAGACGCCTGGC-3' and 5'-CCGCAGGTGGAACAGCTGC-3'.

Real-time quantitative PCR reactions were performed on a 7300 Real-time PCR system (ABI) using THUNDERBIRD SYBR qPCR Mix (Toyobo).

Tumorigenicity of cells and histological analysis

Transplantation (xenografts and allografts) was performed by subcutaneous injection of MSCs, mOS, or human OS (5×10^6) cells into 6–8-week-old female BALB/c-*nu/nu* mice (nude mice). The tumorigenicity of cells was assessed according to tumor weight at 1 month (mOS cells) or 2 months (MSCs and human OS cells) after inoculation. Tissues were fixed with 4% paraformaldehyde in PBS, decalcified in Osteosoft (Merck Millipore) at room temperature for 10 days, embedded in paraffin, and cut into 4 μm sections. An anti-c-Myc antibody (sc-764; Santa Cruz Biotechnology) was used for immunodetection on rehydrated sections pretreated with Target Retrieval Solution (S1699; DAKO). The Envision™+ system (HRP/DAB) (K4011; DAKO) was used for visualization.

Micro-CT analysis

μCT analysis was performed using a μCT system (R_mCT; Rigaku Corporation, Tokyo). Data from the scanned slices were used for three-dimensional analysis to calculate femoral morphometric parameters. Trabecular bone parameters were measured on a distal femoral metaphysis. Craniocaudal scans of approximately 2.4 mm (0.5 mm from the growth plate) for 200 slices in 12 μm increments were performed. The cortical bone parameters were measured in the mid-diaphysis of the femur. The threshold of the mineral density was 500 mg/cm^3.

Statistics

All quantitative data are expressed as the mean ± SD. Differences between groups were calculated by unpaired two-tailed Student's t-test for two groups or by one-way analysis of variance for more than two groups. All analyses were performed using Prism 8 (GraphPad software). Survival was analyzed by the Kaplan–Meier method and compared by the log-rank test using the same software. $P < 0.05$ denoted significance. No samples from *in vivo* and *in vitro* experiments were excluded from the analysis.

Declarations

DATA AVAILABILITY

The RNA-seq data of MSCs and mOS cells generated in this study were submitted to DDJB sequence read archive with the accession number DRA012931 and are available online.

ACKNOWLEDGMENTS

We thank I. Taniuchi, A. Berns, and F. W. Alt for providing the Runx3, p53, and Myc flox mouse lines, respectively, and all members of the Biomedical Research Center, Nagasaki University for maintaining mouse lines. This work was supported by KAKENHI/Japan Society for the Promotion of Science (JSPS) grants 18H02972 (K.I.), 19K22724 (K.I.), and 21H03113 (K.I.), and by the Funding Program for Next Generation World-Leading Researchers LS097 (K.I.).

AUTHOR CONTRIBUTIONS

K.O. and K.I. initiated the study. K.I. designed the experiments. K.O., S.O., Y.D., T.U., T.I., and K.I. conducted the experiments. Y.D. performed bioinformatic analyses. S.O. and K.I. wrote the manuscript. M.U. coordinated the project. K.I. supervised the study.

COMPETING INTERESTS

The authors declare no competing interests.

References

1. Kansara M, Teng MW, Smyth MJ, Thomas DM. Translational biology of osteosarcoma. Nat Rev Cancer 2014; 14: 722–35.
2. Chen X, Bahrami A, Pappo A, Easton J, Dalton J, Hedlund E *et al.* Recurrent somatic structural variations contribute to tumorigenesis in pediatric osteosarcoma. Cell Reports 2014; 7: 104–12.
3. Porter DE, Holden ST, Steel CM, Cohen BB, Wallace MR, Reid R. A significant proportion of patients with osteosarcoma may belong to Li-Fraumeni cancer families. J Bone Jt Surg Br Volume 1992; 74: 883–6.
4. Walkley CR, Qudsi R, Sankaran VG, Perry JA, Gostissa M, Roth SI *et al.* Conditional mouse osteosarcoma, dependent on p53 loss and potentiated by loss of Rb, mimics the human disease. Gene Dev 2008; 22: 1662–76.
5. Berman SD, Calo E, Landman AS, Danielian PS, Miller ES, West JC *et al.* Metastatic osteosarcoma induced by inactivation of Rb and p53 in the osteoblast lineage. Proc National Acad Sci 2008; 105: 11851–11856.
6. Jain M, Arvanitis C, Chu K, Dewey W, Leonhardt E, Trinh M *et al.* Sustained Loss of a Neoplastic Phenotype by Brief Inactivation of MYC. Science 2002; 297: 102–104.
7. Otani S, Date Y, Ueno T, Ito T, Kajikawa S, Omori K *et al.* Runx3 is required for oncogenic Myc upregulation in p53-deficient osteosarcoma. Oncogene 2022; 41: 683–691.
8. Date Y, Ito K. Oncogenic RUNX3: A Link between p53 Deficiency and MYC Dysregulation. Mol Cells 2020; 43: 176–181.

9. Hong J-H, Hwang ES, McManus MT, Amsterdam A, Tian Y, Kalmukova R *et al.* TAZ, a Transcriptional Modulator of Mesenchymal Stem Cell Differentiation. Science 2005; 309: 1074–1078.
10. Rosen ED, Walkey CJ, Puigserver P, Spiegelman BM. Transcriptional regulation of adipogenesis. Gene Dev 2000; 14: 1293–1307.
11. Rosen ED, MacDougald OA. Adipocyte differentiation from the inside out. Nat Rev Mol Cell Bio 2006; 7: 885–896.
12. Wang ND, Finegold MJ, Bradley A, Ou CN, Abdelsayed SV, Wilde MD *et al.* Impaired energy homeostasis in C/EBP alpha knockout mice. Sci New York N Y 1995; 269: 1108–12.
13. Lourenço AR, Coffer PJ. A tumor suppressor role for C/EBPα in solid tumors: more than fat and blood. Oncogene 2017; 36: 5221–5230.
14. Rubio R, Gutierrez-Aranda I, Sáez-Castillo AI, Labarga A, Rosu-Myles M, Gonzalez-Garcia S *et al.* The differentiation stage of p53-Rb-deficient bone marrow mesenchymal stem cells imposes the phenotype of in vivo sarcoma development. Oncogene 2013; 32: 4970–4980.
15. Shimizu T, Ishikawa T, Sugihara E, Kuninaka S, Miyamoto T, Mabuchi Y *et al.* c-MYC overexpression with loss of Ink4a/Arf transforms bone marrow stromal cells into osteosarcoma accompanied by loss of adipogenesis. Oncogene 2010; 29: 5687–5699.
16. Rodriguez R, Rubio R, Menendez P. Modeling sarcomagenesis using multipotent mesenchymal stem cells. Cell Res 2012; 22: 62–77.
17. Hiebert SW, Lipp M, Nevins JR. E1A-dependent trans-activation of the human MYC promoter is mediated by the E2F factor. Proc National Acad Sci 1989; 86: 3594–3598.
18. Johansen LM, Iwama A, Lodie TA, Sasaki K, Felsher DW, Golub TR *et al.* c-Myc is a critical target for c/EBPalpha in granulopoiesis. Mol Cell Biol 2001; 21: 3789–806.
19. Iakova P, Awad SS, Timchenko NA. Aging Reduces Proliferative Capacities of Liver by Switching Pathways of C/EBPα Growth Arrest. Cell 2003; 113: 495–506.
20. Wang H, Goode T, Iakova P, Albrecht JH, Timchenko NA. C/EBPα triggers proteasome-dependent degradation of cdk4 during growth arrest. Embo J 2002; 21: 930–941.
21. Wang H, Iakova P, Wilde M, Welm A, Goode T, Roesler WJ *et al.* C/EBPα Arrests Cell Proliferation through Direct Inhibition of Cdk2 and Cdk4. Mol Cell 2001; 8: 817–828.
22. Ma Y, Kurtyka CA, Boyapalle S, Sung S-S, Lawrence H, Guida W *et al.* A Small-Molecule E2F Inhibitor Blocks Growth in a Melanoma Culture Model. Cancer Res 2008; 68: 6292–6299.
23. Zhang DE, Hetherington CJ, Meyers S, Rhoades KL, Larson CJ, Chen HM *et al.* CCAAT enhancer-binding protein (C/EBP) and AML1 (CBF alpha2) synergistically activate the macrophage colony-stimulating factor receptor promoter. Mol Cell Biol 1996; 16: 1231–1240.
24. Fujimoto T, Anderson K, Jacobsen S, Nishikawa S, Nerlov C. Cdk6 blocks myeloid differentiation by interfering with Runx1 DNA binding and Runx1-C/EBPα interaction. Embo J 2007; 26: 2361–2370.
25. Chuang LSH, Ito K, Ito Y. RUNX family: Regulation and diversification of roles through interacting proteins. Int J Cancer 2013; 132: 1260–1271.

26. Gutierrez S, Javed A, Tennant DK, Rees M van, Montecino M, Stein GS *et al.* CCAAT/Enhancer-binding Proteins (C/EBP) β and δ Activate Osteocalcin Gene Transcription and Synergize with Runx2 at the C/EBP Element to Regulate Bone-specific Expression*. J Biol Chem 2002; 277: 1316–1323.
27. Illendula A, Gilmour J, Grembecka J, Tirumala VSS, Boulton A, Kuntimaddi A *et al.* Small Molecule Inhibitor of CBFβ-RUNX Binding for RUNX Transcription Factor Driven Cancers. Ebiomedicine 2016; 8: 117–131.
28. Chen W, Zhu G, Hao L, Wu M, Ci H, Li Y-P. C/EBPα regulates osteoclast lineage commitment. Proc National Acad Sci 2013; 110: 7294–7299.
29. Lin PP, Pandey MK, Jin F, Raymond AK, Akiyama H, Lozano G. Targeted mutation of p53 and Rb in mesenchymal cells of the limb bud produces sarcomas in mice. Carcinogenesis 2009; 30: 1789–1795.
30. Walkley CR, Qudsi R, Sankaran VG, Perry JA, Gostissa M, Roth SI *et al.* Conditional mouse osteosarcoma, dependent on p53 loss and potentiated by loss of Rb, mimics the human disease. Gene Dev 2008; 22: 1662–76.
31. Porse BT, Pedersen TÅ, Xu X, Lindberg B, Wewer UM, Friis-Hansen L *et al.* E2F Repression by C/EBPα Is Required for Adipogenesis and Granulopoiesis In Vivo. Cell 2001; 107: 247–258.
32. Wurm AA, Zjablovskaja P, Kardosova M, Gerloff D, Bräuer-Hartmann D, Katzerke C *et al.* Disruption of the C/EBPα—miR-182 balance impairs granulocytic differentiation. Nat Commun 2017; 8: 46.
33. Zhao Y, Yu Z, Ma R, Zhang Y, Zhao L, Yan Y *et al.* lncRNA-Xist/miR-101-3p/KLF6/C/EBPα axis promotes TAM polarization to regulate cancer cell proliferation and migration. Mol Ther Nucleic Acids 2020; 23: 536–551.
34. Bennett KL, Hackanson B, Smith LT, Morrison CD, Lang JC, Schuller DE *et al.* Tumor Suppressor Activity of CCAAT/Enhancer Binding Protein α Is Epigenetically Down-regulated in Head and Neck Squamous Cell Carcinoma. Cancer Res 2007; 67: 4657–4664.
35. Seifeddine R, Dreiem A, Blanc E, Fulchignoni-Lataud M-C, Belda M-ALF, Lecuru F *et al.* Hypoxia Down-regulates CCAAT/Enhancer Binding Protein-α Expression in Breast Cancer Cells. Cancer Res 2008; 68: 2158–2165.
36. Lourenço AR, Roukens MG, Seinstra D, Frederiks CL, Pals CE, Vervoort SJ *et al.* C/EBP is crucial determinant of epithelial maintenance by preventing epithelial-to-mesenchymal transition. Nat Commun 2020; 11: 785.
37. Antonson P, Pray MG, Jacobsson A, Xanthopoulos KG. Myc Inhibits CCAAT/Enhancer-Binding Protein α-Gene Expression in HIB-1B Hibernoma Cells Through Interactions with the Core Promoter Region. Eur J Biochem 1995; 232: 397–403.
38. He B-C, Chen L, Zuo G-W, Zhang W, Bi Y, Huang J *et al.* Synergistic Antitumor Effect of the Activated PPARγ and Retinoid Receptors on Human Osteosarcoma. Clin Cancer Res 2010; 16: 2235–2245.
39. Jeon MJ, Kim JA, Kwon SH, Kim SW, Park KS, Park S-W *et al.* Activation of Peroxisome Proliferator-activated Receptor-γ Inhibits the Runx2-mediated Transcription of Osteocalcin in Osteoblasts*. J Biol Chem 2003; 278: 23270–23277.

40. Martin JW, Zielenska M, Stein GS, Wijnen AJ van, Squire JA. The Role of RUNX2 in Osteosarcoma Oncogenesis. *Sarcoma* 2010; 2011: 282745.
41. Shin MH, He Y, Marrogi E, Piperdi S, Ren L, Khanna C *et al.* A RUNX2-Mediated Epigenetic Regulation of the Survival of p53 Defective Cancer Cells. Plos Genet 2016; 12: e1005884.
42. Puig-Kröger A, Sánchez-Elsner T, Ruiz N, Andreu EJ, Prosper F, Jensen UB *et al.* RUNX/AML and C/EBP factors regulate CD11a integrin expression in myeloid cells through overlapping regulatory elements. Blood 2003; 102: 3252–3261.
43. Date Y, Taniuchi I, Ito K. Oncogenic Runx1–Myc axis in p53-deficient thymic lymphoma. Gene 2022; 819: 146234.
44. Jonkers J, Meuwissen R, Gulden H van der, Peterse H, Valk M van der, Berns A. Synergistic tumor suppressor activity of BRCA2 and p53 in a conditional mouse model for breast cancer. Nat Genet 2001; 29: 418–425.
45. Naoe Y, Setoguchi R, Akiyama K, Muroi S, Kuroda M, Hatam F *et al.* Repression of interleukin-4 in T helper type 1 cells by Runx/Cbfβ binding to the Il4 silencer. J Exp Medicine 2007; 204: 1749–1755.
46. Alboran IM de, O'Hagan RC, Gärtner F, Malynn B, Davidson L, Rickert R *et al.* Analysis of C-MYC Function in Normal Cells via Conditional Gene-Targeted Mutation. Immunity 2001; 14: 45–55.
47. Sanjana NE, Shalem O, Zhang F. Improved vectors and genome-wide libraries for CRISPR screening. Nat Methods 2014; 11: 783–784.
48. Ito K, Inoue K, Bae S-C, Ito Y. Runx3 expression in gastrointestinal tract epithelium: resolving the controversy. Oncogene 2009; 28: 1379–1384.

Figures

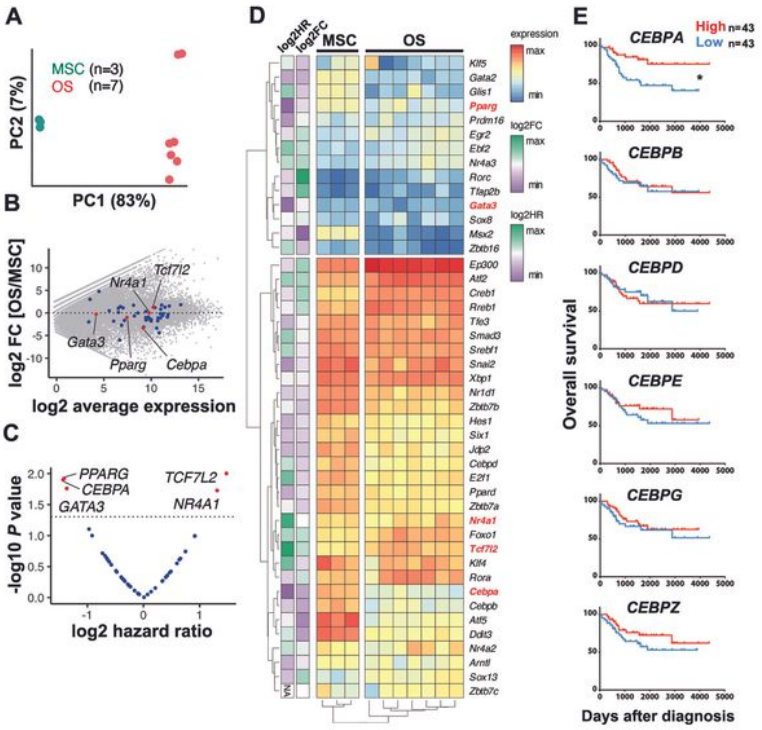

Figure 1

Figure 1

C/ebpα is downregulated in *p53*-deficient osteosarcomagenesis and is a favorable prognostic factor in OS.

(A) Principal component analysis of RNA-seq data comparing OS tissues (OS) and BM-MSCs (MSC) of *OS* mice. (B) MA plot presentation of RNA-seq data comparing OS and MSC. The 45 adipo-TFs are

indicated by dots; five TFs identified as prognostic factors as shown in (C) are indicated by red. (C) Volcano plot of the hazard ratio values for the 45 adipo-TFs calculated based on the TARGET data. Details of (B) and (C) are shown in Supplementary Fig. 1. (D) Heatmap showing color-coded expression levels of adipo-TFs in three MSCs (MSC) and seven OS tissues (OS) from *OS* mice. The hazard ratio values (C) and the gene expression ratio of OS to MSC (B) are shown as log2HR and log2FC, respectively. (E) Prognostic value of *C/EBP*family genes as determined by Kaplan–Meier analysis of survival in OS patients from the TARGET cohort. *p = 0.013.

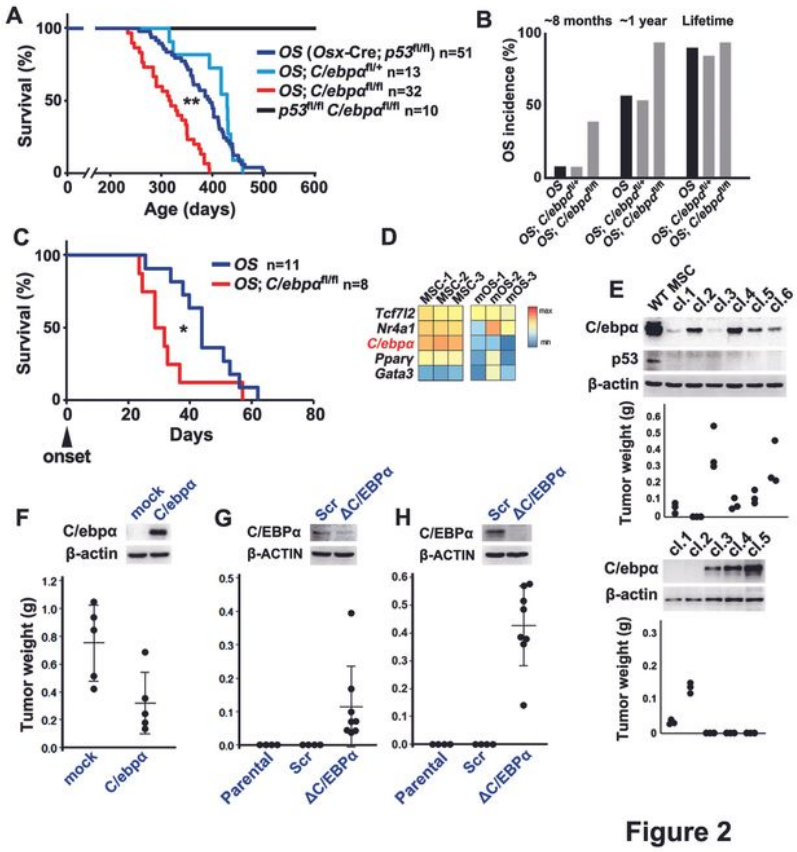

Figure 2

Figure 2

C/ebpα is a tumor suppressor in *p53*-deficient OS.

(A) Survival of *C/ebpa*$^{+/+}$, *C/ebpα*$^{fl/+}$, and *C/ebpα*$^{fl/fl}$ mice in the *OS* (*Osx*-Cre; *p53*$^{fl/fl}$) background, alongside Cre-free controls. (B) Incidence of OS in the indicated genotypes at 8 months and 1 year and throughout the lifespan. (C) Survival of *OS* and *OS*; *C/ebpα*$^{fl/fl}$ mice after the onset of OS. (D) Heatmap showing color-coded expression levels of five prognostic adipo-TFs in three sets of MSCs and mOS cells isolated from three individual *OS* mice. (E) Western blot analysis of the indicated proteins in clonal mOS cells isolated from OS formed in two individual *OS* mice (upper and lower) and MSC from a 1-year-old wild-type mouse (WT MSC). The tumorigenicity of each clone was evaluated by allograft using nude mice (n = 3). (F) Effect of exogenous C/ebpα expression on the tumorigenicity of mOS-1 cells in (D). (G and H) Effect of *C/EBPα* deletion on the tumorigenicity of MG-63 (G) and HS-Os-1 (H) cells. Two types of sgRNAs (h5 and h6; see MATERIALS AND METHODS) were used to deplete C/EBPα, and cells established from each were mixed and evaluated (G, H).

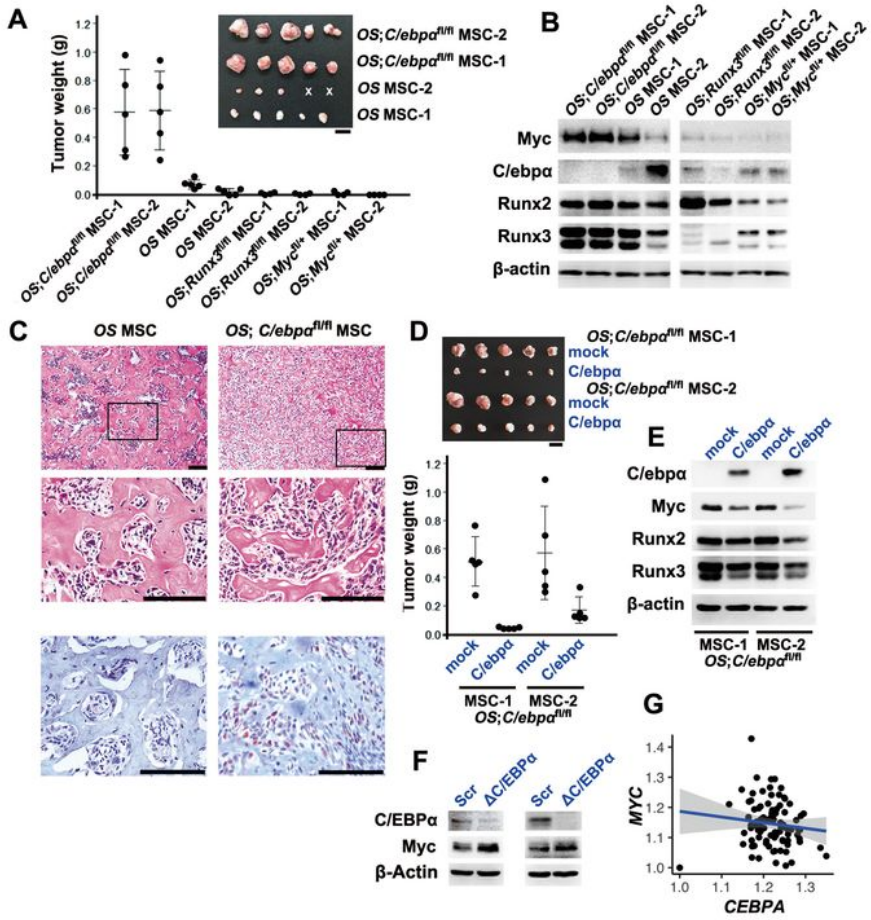

Figure 3

Figure 3

C/ebpa deletion upregulates Myc and enhances the tumorigenicity of *p53*-deficient MSCs (*OS* MSCs).

(A) Tumorigenicity of BM-MSCs (MSCs) from two individuals of each mouse line, *OS;C/ebpa*$^{fl/fl}$ (n = 5), *OS* (n = 5), *OS;Runx3*$^{fl/fl}$ (n = 4), and *OS;Myc*$^{fl/+}$ (n = 4), as evaluated by allograft using nude mice. A photo shows tumors formed by MSCs from *OS;C/ebpa*$^{fl/fl}$ and *OS* mice. (B) Western blot analysis of the

indicated proteins in MSCs used in (A). (C) Representative histology of tumors formed from MSCs of *OS* and *OS;C/ebpα*$^{fl/fl}$ mice (HE; upper) and immunodetection of Myc (lower). Boxed regions are enlarged below (upper). Counter-staining was performed with hematoxylin (lower). (D) Effect of exogenous C/ebpα re-expression on the tumorigenicity of MSCs from *OS;C/ebpα*$^{fl/fl}$ mice. The tumorigenicity was evaluated by allograft using nude mice (n = 5). A photo shows tumors formed. (E) Western blot analysis of the indicated proteins in MSCs used in (D). (F) Western blot analysis of Myc expression in MG-63 (left) and HS-Os-1 (right) cells used in Fig. 2G, H. Blots for C/EBPα and β-Actin are identical to those in Fig. 2G. (G) *MYC* expression levels plotted against *C/EBPα* expression levels in human OS (TARGET; n = 89). Spearman rank correlation coefficient: -0.1801. p = 0.0456. Scale bars = 1 cm (A, D) and 100 μm (C).

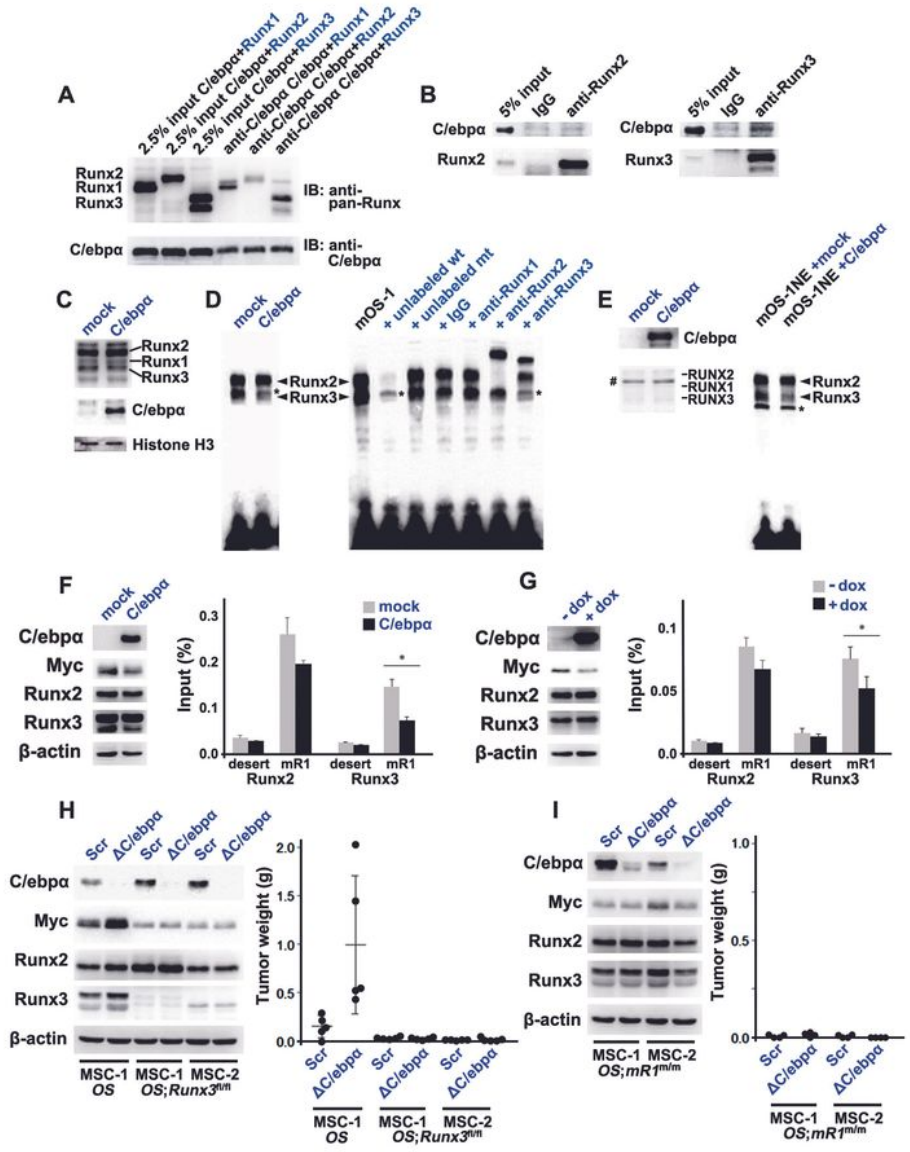

Figure 4

Figure 4

C/ebpα decreases the DNA binding of Runx3 to mR1 in the absence of p53.

(A) Immunoprecipitates of whole-cell extracts of 293T cells expressing exogenous C/ebpα and Runx1, Runx2, or Runx3 with anti-C/ebpα antibody were subjected to western blotting. (B) Immunoprecipitates of NE of *OS* MSCs generated with anti-Runx2 (left) or anti-Runx3 (right) antibody or normal rabbit IgG were

subjected to western blotting. (C) Amounts of the indicated proteins in nuclear extracts (NEs) of mOS-1 cells shown in Fig. 2D expressing mock or exogenous C/ebpα. Runx1, Runx2, and Runx3 proteins were detected using an anti-pan-Runx antibody. (D) EMSA using NEs shown in (C) and a labeled DNA probe with an intact mR1 (wt) sequence (left). EMSA using NEs of mOS-1 cells and a labeled wt probe, unlabeled wt or mutated mR1 (mt) probe, and normal IgG, anti-Runx1, anti-Runx2, or anti-Runx3 antibody (right). The positions of probe-Runx2 and -Runx3 complexes are indicated. (E) The NE of mOS-1 cells was mixed with the NE of 293T cells expressing mock or exogenous C/ebpα, and then subjected to EMSA using a labeled wt probe (right). Western blot analysis of exogenous C/ebpα and undetectable levels of endogenous RUNX1, RUNX2, and RUNX3 in NEs of 293T cells added to the EMSA (left). Asterisks (*) show the position of non-specific shift bands (D, E). # shows non-specific bands (E). (F) Western blot analysis of the indicated proteins in mOS-2 cells (Fig. 2D) expressing mock or exogenous C/ebpα (left). Occupancy of Runx2 and Runx3 on mR1 in those cells as assessed by ChIP (right). (G) Western blot analysis of the indicated proteins in *p53*-deleted ST2 cells with or without induction of C/ebpα by doxycycline (dox) (left). Occupancy of Runx2 and Runx3 on mR1 in those cells, as assessed by ChIP (right). A gene-desert region of the mouse genome (desert) was used as a negative control for all ChIP assays (n=3). *$p < 0.05$ (F, G). (H) Western blot analysis of the indicated proteins in *OS* MSCs and *OS*;*Runx3*$^{fl/fl}$ MSCs with or without endogenous C/ebpα (left) and their tumorigenicity evaluated by allograft using nude mice (n = 5) (right). (I) Western blot analysis of the indicated proteins in *OS*;*mR1*$^{m/m}$ MSCs generated from *OS*; *mR1*$^{m/m}$ mice[7] with or without endogenous C/ebpα (left) and their tumorigenicity evaluated by allograft using nude mice (n = 4) (right).

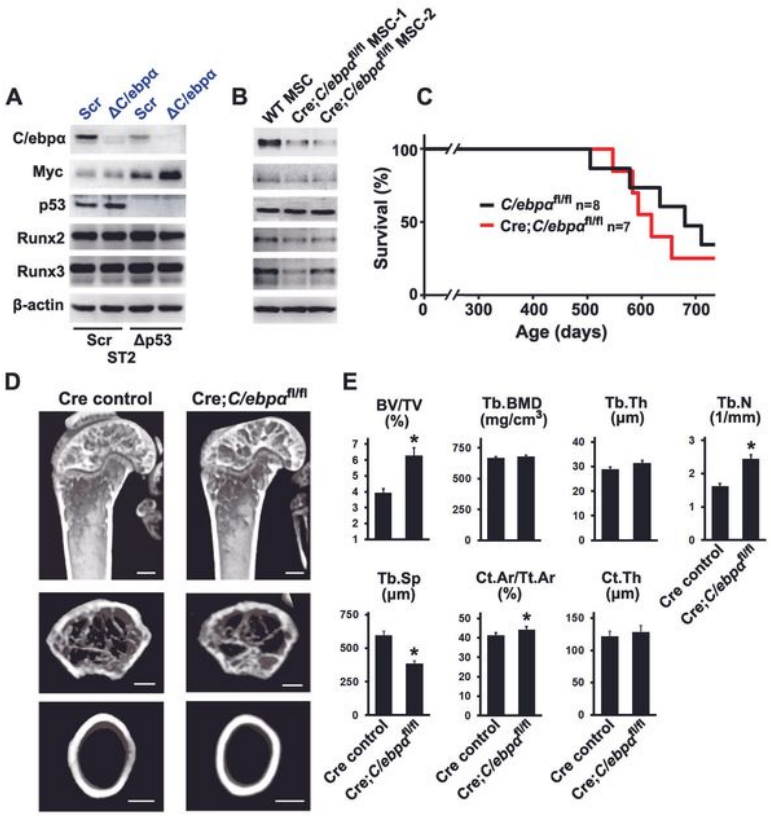

Figure 5

Figure 5

C/ebpα deletion does not affect Myc expression and osteosarcomagenesis in the presence of p53.

(A) Western blot analysis of the indicated proteins in control or *p53*-deleted ST2 cells with or without endogenous C/ebpα. (B) Western blot analysis of the indicated proteins in MSCs generated from a wild-type (WT) mouse and *Osx*-Cre;*C/ebpα*$^{fl/fl}$ mice. (C) Survival of *C/ebpα*$^{fl/fl}$ and *Osx*-Cre;*C/ebpα*$^{fl/fl}$ mice. (D)

Representative μCT three- or two-dimensional images of the bone architecture of male *Osx*-Cre;*C/ebpa*$^{fl/fl}$ and *Osx*-Cre (Cre control) mice at 10 weeks of age. Images of trabecular bone in the distal femoral metaphysis (upper and middle) and cortical bone at mid-diaphysis in femurs (lower) are shown. (E) Quantification of the trabecular bone volume (bone volume/tissue volume, BV/TV), trabecular bone mineral density (Tb.BMD), trabecular thickness (Tb.Th), trabecular number (Tb.N), trabecular separation (Tb.Sp), cortical area (Ct.Ar/Tt.Ar), and cortical thickness (Ct.Th) in *Osx*-Cre;*C/ebpa*$^{fl/fl}$ and Cre control mice (n = 3). Scale bars = 500 μm (D).

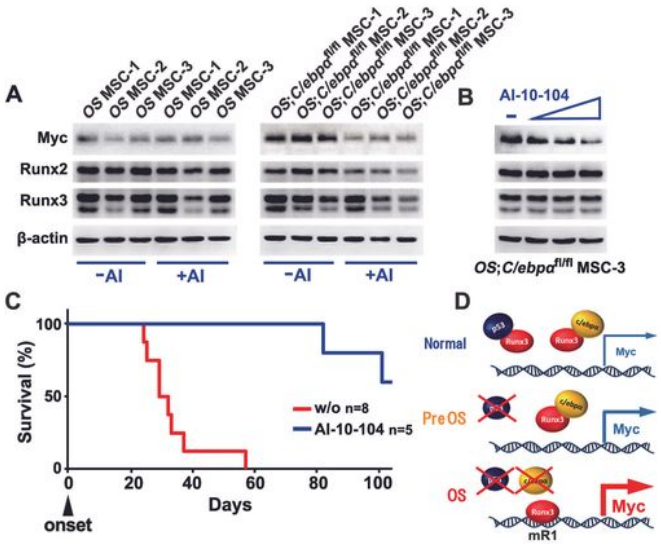

Figure 6

Figure 6

Runx inhibitors have therapeutic effects on *p53*- and *C/ebpα*-deficient OS.

(A) Western blot analysis of the indicated proteins in *OS* and *OS*; *C/ebpa*$^{fl/fl}$ MSCs treated with or without AI-10-104 (10 μM for 24 h). (B) Western blot analysis of the effect of AI-10-104 (0, 2, 6, or 10 μM for 24 h) on Myc expression in *OS*; *C/ebpa*$^{fl/fl}$ MSC-3 used in (A). (C) Survival of *OS*; *C/ebpa*$^{fl/fl}$ mice treated with or

without (w/o) AI-10-104 for 90 days after the onset of OS. The survival curve for w/o mice is identical to that in Fig. 2C. (D) C/ebpα as well as p53 attenuate Runx3 DNA binding, thereby suppressing aberrant Myc upregulation (upper). The *p53*-negative MSCs, in which only C/ebpα attenuates Runx3, are considered to be 'Pre-OS' (middle). In OS, Runx3 unleashed from both p53 and C/ebpα strongly upregulates Myc (lower).

Supplementary Files

This is a list of supplementary files associated with this preprint. Click to download.

- SuppleOmorietalsubmission.docx